(1970).
[10]T. Sagawa *et al.*, J. Phys. Soc. Japan 21, 2587 (1966).
[11]A. B. Kunz, Phys. Rev. 175, 1147 (1968).
[12]A. B. Kunz, Phys. Status Solidi 29, 115 (1968).
[13]A. B. Kunz, J. Phys. Chem. Solids 31, 265 (1970).
[14]L. J. Page and E. H. Hygh, Phys. Rev. B 1, 3472 (1970).
[15]P. D. DeCicco, Phys. Rev. 153, 931 (1967).
[16]C. Y. Fong and M. L. Cohen, Phys. Rev. 185, 1168 (1969).
[17]Y. Onodera, M. Okazaki, and T. Inui, J. Phys. Soc. Japan 21, 2229 (1966).
[18]H. Overhof, Phys. Status Solidi 43b, 575 (1971).
[19]D. G. Shankland, Boeing Document No. D6-29730, The Boeing Company, Renlon, Wash. (unpublished).
[20]R. N. Euwema *et al.*, Phys. Rev. 178, 1419 (1969).
[21]G. Dresselhaus and M. S. Dresselhaus, Phys. Rev. 160, 649 (1967).
[22]F. Herman, R. L. Kortum, C. D. Kuglin, and J. L. Shay, *II-VI Semiconducting Compounds*, 1967 *International Conference*, edited by D. G. Thomas (Benjamin, New York, 1967), pp. 503—551.
[23]F. Herman, R. L. Kortum, C. D. Kuglin, and R. A. Short, *Quantum Theory of Atoms, Molecules and the Solid State*, edited by P.-O. Löwdin (Academic, New York, 1966), p. 381.
[24]F. Herman and S. Skillman, *Atomic Structure Calculations* (Prentice Hall, Englewood Cliffs, N. J., 1963).
[25]K. Siegbahn *et al.*, *ESCA* (Almquist and Wiksells, Uppsala, 1967).
[26]H. M. O'Brian and H. W. B. Skinner, Proc. Roy. Soc. (London) A176, 229 (1940).
[27]S. Nakai and T. Sagawa, J. Phys. Soc. Japan 26, 1427 (1969).

PHYSICAL REVIEW B VOLUME 5, NUMBER 10 15 MAY 1972

Raman Scattering in Paratellurite, TeO_2 †

A. S. Pine and G. Dresselhaus
Lincoln Laboratory, Massachusetts Institute of Technology, Lexington, Massachusetts 02173
(Received 13 December 1971)

Raman spectra of the tetragonal D_4^4 structure of TeO_2, paratellurite, have been obtained at temperatures of 85 and 295 °K. Frequencies and symmetry assignments for 18 of the 21 Raman-active optical branches are given with only one singlet-A_1 and two doublet-E modes not observed. The measured LO-TO splittings of the six E modes observed accounts for 63% of the total oscillator strength of the known ionic contribution to the ordinary-ray dielectric constant. Estimates for the positions of the LO and TO branches of the Raman-inactive, infrared-active, A_2 modes are made from the anisotropic frequency shifts of the oblique phonons in the extraordinary ray. In addition some weak, anomalous, polarization-selection-rule violations are reported.

I. INTRODUCTION

Tellurium dioxide exists in three stable crystalline forms[1]: one orthorhombic, D_{2h}^{15} (known as tellurite), and two tetragonal, D_4^4 (known as paratellurite) and D_{4h}^{14} (isomorphous to rutile). Of these, paratellurite, which has been synthesized in rather large specimens,[2-4] lacks a center of inversion and is optically active.[5-7] Paratellurite is transparent from 0.33 to 6.5 μm with high and strongly birefringent refractive indices[2,6] ($n_0 = 2.274$ and $n_e = 2.430$ at 0.589 μm), and it has elastic constants which result in an extremely slow ⟨110⟩ shear wave.[8-10] These characteristics lead to interesting piezoelectric,[8-10] acousto-optic[11] and nonlinear optical[4] applications. Useful application may also be found for the optical phonon properties reported here.

The Raman spectrum of paratellurite has been obtained at 85 and 295 °K. The 25 optical-phonon frequencies and symmetries are given except for one A_1 and two E modes which were not observed. The four A_2 optical branches, which are Raman inactive, are inferred from the frequencies of the mixed $A_2 + E$ extraordinary phonons. Several of the Raman peaks are very strong and sharp compared to similar oxides such as rutile and α-quartz which indicates relatively large polarizabilities and weak anharmonic forces.

II. MODE SYMMETRIES AND POLARIZATIONS

The unit cell of paratellurite contains four TeO_2 molecules resulting in 36 phonon branches with Γ-point symmetries $4A_1 + 5A_2 + 5B_1 + 4B_2 + 9E$. Of these $1A_2 + 1E$ comprise the acoustic modes; the singlet-A_2 modes are infrared active in the extraordinary ray, and the doublet-E modes are infrared active in the ordinary ray. All the optical branches are Raman active except for the pure A_2 modes. The Raman polarization selection rules for D_4 symmetry have been given by Loudon[12]:

$$\underline{\alpha}(A_1) = \begin{pmatrix} a & . & . \\ . & a & . \\ . & . & b \end{pmatrix}, \quad \underline{\alpha}(B_1) = \begin{pmatrix} c & . & . \\ . & -c & . \\ . & . & . \end{pmatrix},$$

$$\underline{\alpha}(B_2)=\begin{pmatrix} . & d & . \\ d & . & . \\ . & . & . \end{pmatrix},$$

$$\underline{\alpha}(E_x)=\begin{pmatrix} . & . & . \\ . & . & e \\ . & e & . \end{pmatrix}, \quad \underline{\alpha}(E_y)=\begin{pmatrix} . & . & -e \\ . & . & . \\ -e & . & . \end{pmatrix}.$$

Of course Raman scattering probes phonons at small, but finite, wave vector $\vec{q}$. For $\vec{q}\perp\vec{c}$ axis the electromagnetic field splits the longitudinal and transverse polarizations of the E modes[12]; for $\vec{q}\parallel\vec{c}$ axis the E modes are split proportional to wave vector into oppositely circular polarized branches[13]; for $\vec{q}$ at a general angle to the c axis the E and A_2 modes are mixed in the extraordinary polarization.[14,15] The dielectric constant for the ordinary ray, ignoring damping, is

$$\epsilon_0(\omega)=\epsilon_0(\infty)+\sum_{i=1}^{8}\frac{f_{E_i}}{1-(\omega/\omega_{E_{\mathrm{TO}i}})^2}, \tag{1}$$

and for the extraordinary ray

$$\epsilon_e(\omega)=\epsilon_e(\infty)+\sum_{i=1}^{4}\frac{f_{A_{2i}}}{1-(\omega/\omega_{A_{2\mathrm{TO}i}})^2}. \tag{2}$$

Here the f_i are the mode oscillator strengths, $\omega_{\mathrm{TO}i}$ are the frequencies of the transverse-polarized modes, and $\epsilon(\infty)$ are the squares of the optical refractive indices. The zeros of the dielectric constants yield the LO frequencies. Thus the coupled equations[16]

$$0=\epsilon_0(\infty)+\sum_{i=1}^{8}\frac{f_{E_i}}{1-(\omega_{E_{\mathrm{LO}j}}/\omega_{E_{\mathrm{TO}i}})^2}, \quad i=1,2,\ldots,8 \tag{3}$$

relate the oscillator strengths to the LO-TO frequencies. The dc ordinary dielectric constant may be obtained from (1),

$$\epsilon_0(0)=\epsilon_0(\infty)+\sum_{i=1}^{8}f_{E_i}, \tag{4}$$

or from the generalized Lyddane-Sachs-Teller relations

$$\epsilon_0(0)/\epsilon_0(\infty)=\prod_{i=1}^{8}(\omega_{E_{\mathrm{LO}i}}/\omega_{E_{\mathrm{TO}i}})^2. \tag{5}$$

Similar expressions hold for $\omega_{A_{2\mathrm{LO}i}}$ and $\epsilon_e(0)$.

If the phonon wave vector makes an angle θ with the c axis, the extraordinary-ray dielectric constant is given by[14]

$$\epsilon_\theta(\omega)=\epsilon_0(\omega)\epsilon_e(\omega)/[\epsilon_e(\omega)\cos^2\theta+\epsilon_0(\omega)\sin^2\theta]. \tag{6}$$

The peaks in the Raman spectra occur at the poles of $\epsilon_\theta(\omega)$, or equivalently at the zeros of the bracketed denominator. Thus it is seen that the spectra vary anisotropically with θ and contain information about the A_2 frequencies and oscillator strengths. This angular dispersion of oblique phonons has been observed in a number of crystals.[17]

III. EXPERIMENT

The paratellurite sample was obtained from Arlt and Liebertz of Philips Laboratory, Aachen, Germany. The polished sample faces were oriented normal to the principal crystal axes with dimensions $8\times8\times1.3$ mm along ⟨100⟩, ⟨010⟩, and ⟨001⟩, respectively. The sample was mounted on the cold finger of a liquid-nitrogen Dewar for the data at 85 °K. Raman spectra were recorded using argon-laser excitation at 5145 Å with power of 120 mW, a Spex-1400 double monochromator with 50/100/50 μm slits, and an uncooled FW 130 photomultiplier with ~20 dark counts/sec.

Polarized Raman spectra of paratellurite at 295 and 85 °K are exhibited in Figs. 1 and 2. The conventional $\alpha(\beta\gamma)\delta$ notation for the scattering geometry is employed where α and δ are the incident and scattered directions of the wave vectors and β and γ are the incident and scattered polarizations. The selection rules are indicated on the figures where x, y, and z refer to the ⟨100⟩, ⟨010⟩, and ⟨001⟩ crystal axes. A logarithmic intensity scale (counts/sec) is displayed because of the wide disparities of scattering cross sections between the various modes. The mode identifications for the allowed polarizations are labeled along with their frequency shifts in cm^{-1}. Some of the stronger modes persistently leak into forbidden polarizations and are labeled in parentheses. These selection-rule violations will be discussed later. The mode frequencies and symmetry assignments are collected in Table I. The frequencies are accurate to ±1 cm^{-1}. At 85 °K, one A_1 and two $E_{\mathrm{TO}}+E_{\mathrm{LO}}$ modes are not observed; at 295 °K an additional two E_{TO} modes are lost in the background. The temperature shifts of the phonon frequencies are

TABLE I. Phonon frequencies (cm^{-1}) and symmetries in paratellurite.

	A_1	B_1	B_2	E_{TO}	E_{LO}
295 °K	148	62	155	122	122
	393	175	287	174	197
	648	216	414	···	239
		233	784	297	336
		591		···	718
				766	809
85 °K	152	62	157	123	126
	392	179	281	177	200
	649	218	415	215	239
		235	786	299	340
		589		642	718
				769	811

generally less than 3% and the linewidths of several peaks at 85 °K are narrower than the instrumental resolution of ~1 cm^{-1}. These facts indicate a relatively small anharmonicity.

IV. EXTRAORDINARY-RAY PHONON ANISOTROPY

The Raman spectrum of paratellurite at 85 °K in the geometry $y(z, x+y)z$ is shown in Fig. 3. Here

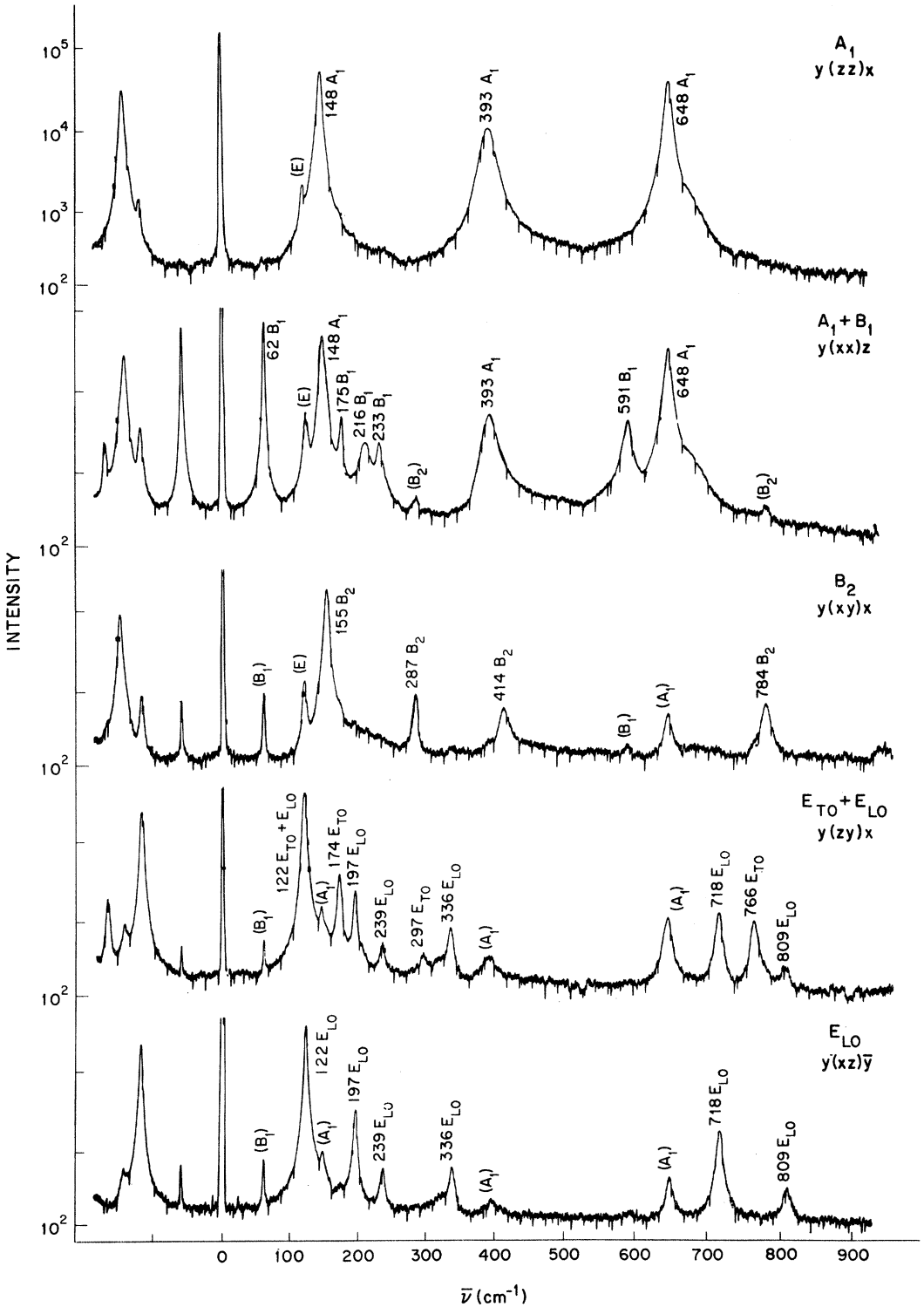

FIG. 1. Survey Raman spectra of paratellurite at 295 °K.

the phonons are propagating along ⟨011⟩. The peaks formerly associated with E_{LO} are shifted to new positions $\tilde{E}_{LO}$ and four new modes, labeled $\tilde{A}_2$, appear. These are the mixed A_2+E extraordinary-ray oblique phonons. The remaining peaks corresponding to E_{TO} and the leakage A_1, B_1, and B_2 modes are

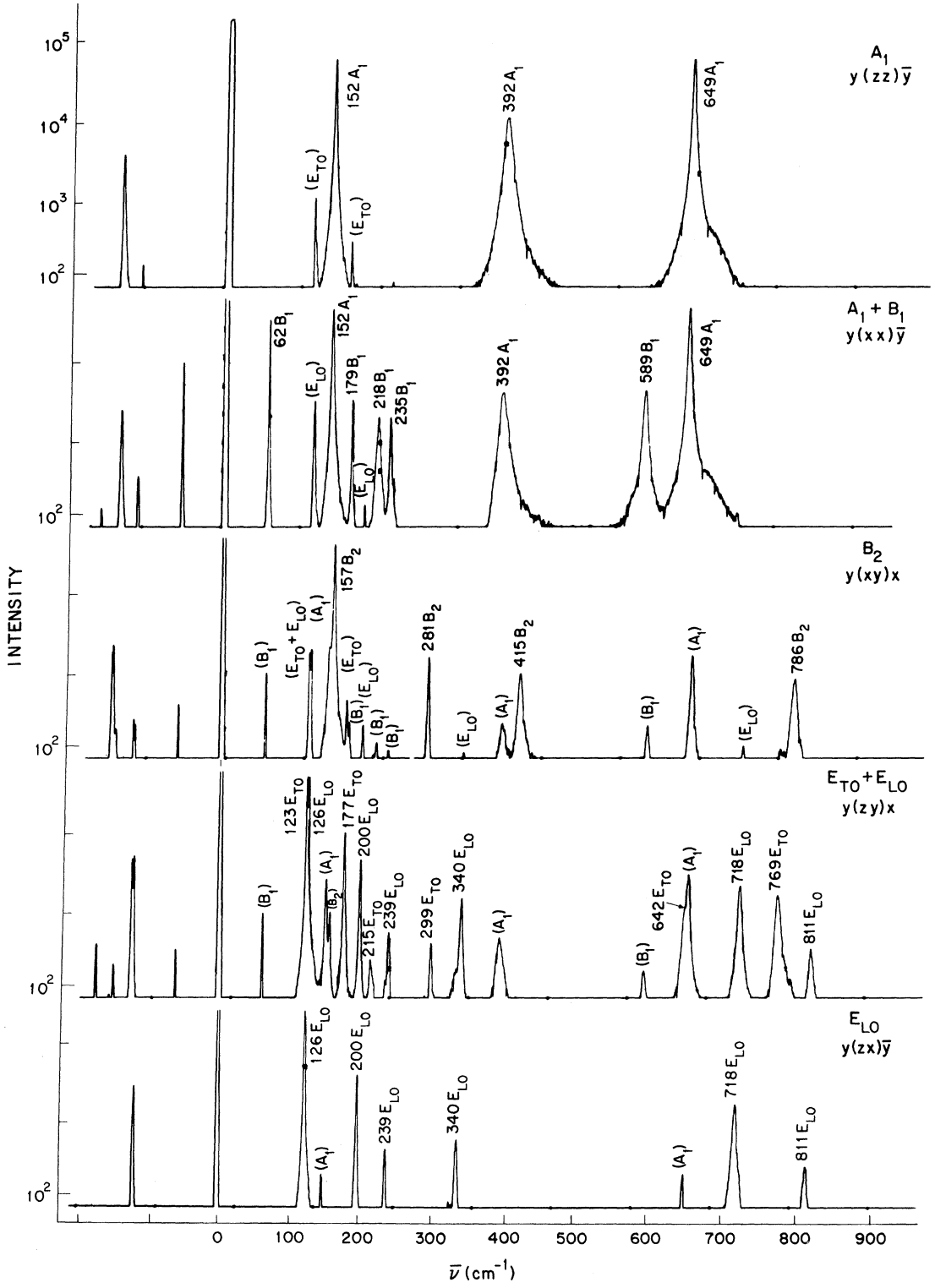

FIG. 2. Survey Raman spectra of paratellurite at 85 °K.

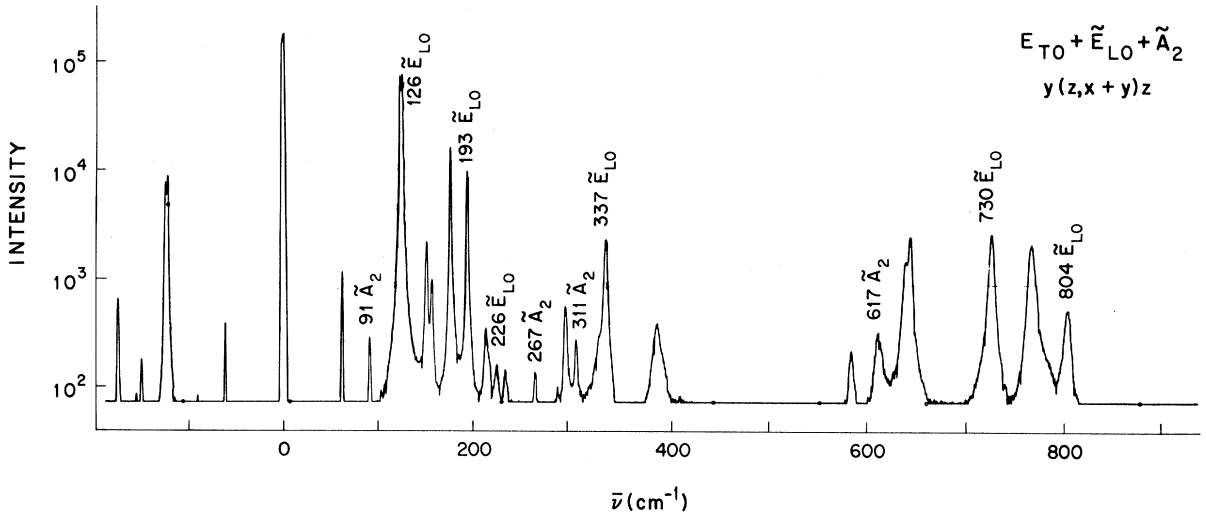

FIG. 3. Raman spectrum of oblique phonons in paratellurite at 85 °K.

unchanged from the $y(zy)x$ trace of Fig. 2.

The measured oblique phonon frequencies are computer fit to the roots of $\epsilon_e(\omega)\cos^2\theta+\epsilon_0(\omega)\sin^2\theta=0$, from Eq. (6) by adjusting the A_2 LO and TO frequencies compatible with the extraordinary dc dielectric constant[8] $\epsilon_e(0)=25$. The measured[8] $\epsilon_0(0)=21.5$ is not used since two contributing E modes are not observed. The experimental E_{LO} and E_{TO} frequencies result in $\epsilon_0(0)=15.5$ according to Eq. (5). The results of the computer fit are collected in Table II where they are compared to the measured ⟨011⟩ data. Since only six E modes are included in $\epsilon_0(\omega)$, the A_2 positions must be considered a rough estimate. However, two trial E modes inserted in the 0–100-cm^{-1} and 400–500-cm^{-1} gaps do not markedly affect the results, so the estimates are probably good to ± 5 cm^{-1}. Using the parameters of Table II, the anisotropic frequencies of the extraordinary-ray phonons are calculated and drawn in Fig. 4. The tuning curves cover a large frequency range for some of these phonons; the Raman cross sections, which depend on the amount of E-mode admixture, vanish as the phonons approach the pure ω_{A_2LO} for $\theta=0°$ or the ω_{A_2TO} for $\theta=90°$. Unfortunately the ordering of the A_2 modes and the assignments of the $\tilde{E}_{LO}$ and $\tilde{A}_2$ are somewhat intuitive so systematic errors are possible. (See note added in proof.) Therefore polarized infrared reflectivity spectra of paratellurite are of interest, both for testing the A_2 assignments and for locating the two missing E modes.

V. ANOMALOUS SELECTION-RULE VIOLATIONS

The modes labeled by parentheses in Figs. 1 and 2 should be forbidden for the polarizations indicated. Such leakage is usually attributed to experimental depolarization or misorientation effects. However, these are probably not responsible for some of the present observations. The incident beam is well polarized but becomes slightly depolarized (<1%) on passing through the sample. This is due to circular birefringence since the normal modes of an optically active crystal are elliptically polarized even for $\vec{q}\perp\langle 001\rangle$.[18] This effect dominates other depolarizing factors such as surface deformation, internal defects and strains, and linear birefringence. However, allowing for depolarization, the $y(zz)\bar{y}$ trace of Fig. 2 should include contributions from $y(xx)\bar{y}\rightarrow B_1$ and $y(zx)\bar{y}\rightarrow E_{LO}$, but not the observed E_{TO}. Similarly the observed B_1 components of the $y(xy)x$ and the $y(zy)x$ traces of Fig. 2 are not expected from simple depolarization. Furthermore, some of the modes which are contained within the

TABLE II. Extraordinary-ray-oblique-phonon frequencies (cm^{-1}) and oscillator strengths in paratellurite at 85 °K.

E_{TO} expt.	E_{LO} expt.	f_E calc.	A_{2TO} calc.	A_{2LO} calc.	f_{A_2} calc.
123	126	0.9	76	109	13.2
177	200	5.0	265	269	0.4
215	239	1.2	325	335	0.8
299	340	1.4	570	785	5.0
642	718	1.6			
769	811	0.2			
	$\tilde{E}_{LO}$	$\tilde{A}_2$	$\tilde{E}_{LO}$	$\tilde{A}_2$	
$\theta=45°$	expt.	expt.	calc.	calc.	
	126	91	126	91	
	193	267	193	268	
	226	311	223	308	
	337	617	336	616	
	730		735		
	804		804		

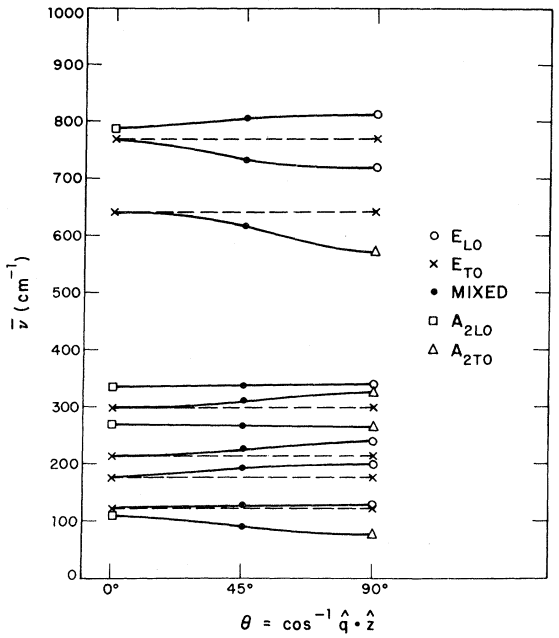

FIG. 4. Angular dispersion of the infrared-active phonons in paratellurite accessible to large-angle Raman scattering. θ is the angle between the c axis and the phonon wave vector. The points labeled E_{LO}, E_{TO}, and mixed are experimental; the points labeled A_{2LO}, A_{2TO}, and the curves are calculated.

depolarized symmetry, such as E_{LO} in $y(xx)\bar{y}$, are more intense than warranted by the degree of depolarization.

Misorientation effects arise from crystal-axis offsets and the finite collection solid angle. However the observed selection-rule violations are insensitive to small crystal rotations or changes in the collection solid angle. The traces displayed were obtained with a collection aperture stop of $f/2.8$ for right-angle scattering and $f/10$ for backscattering. The relative amount of leakage is unaffected when the aperture stop is doubled or halved. Therefore it seems likely that something more fundamental than misorientation or depolarization is causing the leakage. A summary of the principal selection-rule violations is presented in Table III. A variety of morphic effects, such as linear wave-vector-, field-, or strain-induced scattering, have been considered; but none has been found to consistently explain all of the violations.

VI. DISCUSSION

The optical phonons of paratellurite are almost completely determined by Raman scattering. Even the frequencies of the Raman-inactive A_2 branches can be estimated from the positions of the oblique phonons in the extraordinary ray. Only one A_1 and two E modes have not been found. Some interesting selection-rule violations have been observed.

Several of the modes are very intense scatterers, notably the 62-cm^{-1} B_1, 123–126-cm^{-1} E, 152-cm^{-1} A_1, 157-cm^{-1} B_2, and 649-cm^{-1} A_1. These peaks are all about 40 times as intense as the strongest 468-cm^{-1} A_1 mode in α-quartz, and each of these lines except the 649-cm^{-1} A_1 have narrower linewidths than the quartz line.[19] Thus these modes are good candidates for stimulated Raman scattering. Furthermore, stimulated scattering of the weaker infrared-active modes could result in tunable radiation by polariton scattering either in the near-forward configuration[20] or in the extraordinary ray. The very strong scattering peaks of paratellurite have been observed previously by the authors in a Raman study of tellurium.[21] There polycrystalline TeO_2 was created simply by melting and oxidizing the surface with the laser. This stable, dominant spectrum may be expected when other tellurium compounds are examined.

Finally, as mentioned by Wyckoff,[1] the crystal structure of paratellurite D_4^4 is a slight distortion of the rutile D_{4h}^{14} structure doubled in the c direction. Since this implies a folding of the Brillouin zone along the ⟨001⟩ axis, the Γ-point phonon branches of paratellurite should be related to the $\Gamma + Z$ points of the rutile zone.[22] The Raman spectrum may then be expected to be dominated by the allowed Γ-point rutile modes with weaker contributions from Z-point and odd-parity rutile modes turned on by the cell doubling and loss of inversion symmetry. However the strong Raman peaks in paratellurite do not closely resemble the typical pattern observed in many crystals of the rutile family.[23]

Note added in proof. M. Krauzman and J-P. Mathieu [Compt. Rend. 273B, 342 (1971)] have independently studied the phonon spectra of paratellurite, and our results are in general agreement except for a few discrepancies. In the $y(xx)\bar{y}$ spectrum, they identify our 233-cm^{-1} B_1 mode as

TABLE III. Polarization-selection-rule violations in paratellurite.

Experimental geometry	Observed forbidden modes
$y(zz)\bar{y}$	E_{TO}
$x(zz)\bar{x}$	E_{TO}
$y(xx)\bar{y}$	E_{LO}
$x(yy)\bar{x}$	E_{LO}
$y(zz)x$	$E_{LO}+E_{TO}+B_1$
$y(xy)x$	$E_{LO}+E_{TO}+A_1+B_1$
$y(zy)x$	$A_1+B_1+B_2$
$y(zx)\bar{y}$	A_1

A_1 and our 122-cm^{-1} E mode leakage as B_1. Their infrared reflectivity measurements indicate an $A_{2TO} - A_{2LO}$ pair at 315–375 cm^{-1} in place of our 325–335-cm^{-1} pair inferred from the oblique phonon Raman measurement. Our preliminary reflectivity data confirm the larger strength assignment. This A_2 mode is poorly predicted by the Raman technique because of the coupling of the unobserved E modes in this spectral region. Further work is proceeding on the reflectivity of paratellurite in order to test our assignments on the remaining polar phonons.

ACKNOWLEDGMENT

The authors are very grateful to Dr. G. Arlt of Philips Laboratory, Aachen, Germany, who kindly supplied the crystal used in this study.

---

†Work sponsored by the U. S. Department of the Air Force.

[1]R. W. G. Wyckoff, *Crystal Structures* (Interscience, New York, 1963), Vol. 1, pp. 250–257.

[2]J. Liebertz, Kristall. Technik. 4, 221 (1969).

[3]S. Miyazawa and H. Iwasaki, Japan. J. Appl. Phys. 9, 441 (1970).

[4]W. A. Bonner, S. Singh, L. G. Van Uitert, and A. W. Warner, J. Electron. Materials 1, 155 (1972); D. S. Chemla and J. Jerphagnon, Appl. Phys. Letters 20, 222 (1972).

[5]N. Uchida, S. Miyazawa, and S. Saito, J. Phys. Soc. Japan 28, 800 (1970).

[6]N. Uchida, Phys. Rev. B 4, 3736 (1971).

[7]V. Janku and V. Vysin, Optics Commun. 3, 308 (1971).

[8]G. Arlt, J. Liebertz, and H. Schweppe, in Proceedings of the Sixth International Conference on Acoustics, Tokyo, 1968 (unpublished).

[9]G. Arlt and H. Schweppe, Solid State Commun. 6, 783 (1968).

[10]H. Schweppe, Ultrasonics 8, 84 (1970).

[11]N. Uchida and Y. Ohmachi, Japan J. Appl. Phys. 9, 155 (1970).

[12]R. Loudon, Advan. Phys. 13, 423 (1964).

[13]A. S. Pine and G. Dresselhaus, Phys. Rev. 188, 1489 (1969).

[14]R. Loudon, in *Light Scattering Spectra of Solids*, edited by G. B. Wright (Springer-Verlag, New York, 1969), p. 25.

[15]L. Merten, Z. Naturforsch. 22a, 359 (1966).

[16]J. F. Scott, Phys. Rev. B 1, 3488 (1970).

[17]Wurtzites: C. A. Arguello, D. L. Rousseau, and S. P. S. Porto, Phys. Rev. 181, 1351 (1969). $LiIO_3$: W. Otaguro, E. Wiener-Avnear, C. A. Arguello, and S. P. S. Porto, *ibid.* B 4, 4542 (1971). α-quartz: L. Couture-Mathieu, J. A. A. Ketelaar, W. Vedder, and J. Fahrenfort, J. Chem. Phys. 20, 1492 (1952); J. F. Scott, Am. J. Phys. 39, 1360 (1971). Tellurium: W. Richter, Bull. Am. Phys. Soc. 16, 335 (1971); and unpublished. $LiNbO_3$: R. Claus and H. W. Shrotter, in *Light Scattering in Solids*, edited by M. Balkanski (Flammarion, Paris, 1971), p. 244. $NaNO_2$: C. M. Hartwig, E. Wiener-Avnear, J. Smit, and S. P. S. Porto, Phys. Rev. B 3, 2078 (1971).

[18]J. F. Nye, *Physical Properties of Crystals* (Clarendon, Oxford, 1964), Chap. XIV.

[19]A. S. Pine and P. E. Tannenwald, Phys. Rev. 178, 1424 (1969).

[20]C. H. Henry and J. J. Hopfield, Phys. Rev. Letters 15, 964 (1965); J. M. Yarborough, S. S. Sussman, H. E. Puthoff, R. H. Pantell, and B. C. Johnson, Appl. Phys. Letters 15, 102 (1969).

[21]A. S. Pine and G. Dresselhaus, Phys. Rev. B 4, 356 (1971).

[22]This effect has been observed in SiC polytypes by D. W. Feldman, J. H. Parker, W. J. Choyke, and L. Patrick, Phys. Rev. 173, 787 (1968), and in the α-$AlPO_4$/α-SiO_2 system by J. F. Scott, Phys. Rev. B 4, 1360 (1971).

[23]S. P. S. Porto, P. A. Fleury, and T. C. Damen, Phys. Rev. 154, 522 (1967); J. F. Scott, J. Chem. Phys. 53, 852 (1970); and Ref. 16.